AJNR Am J Neuroradiol 23:1038–1048, June/July 2002

Posterior Reversible Encephalopathy Syndrome: Prognostic Utility of Quantitative Diffusion-Weighted MR Images

Diego J. Covarrubias, Patrick H. Luetmer, and Norbert G. Campeau

BACKGROUND AND PURPOSE: **The recently described posterior reversible encephalopathy syndrome (PRES) classically consists of reversible vasogenic edema in the posterior circulation territories, although conversion to irreversible cytotoxic edema has been described. We hypothesized that the extent of edema has prognostic implications and that diffusion-weighted MR imaging (DWI) can help predict the progression to infarction.**

***METHODS*: Twenty-two patients with PRES and 18 control subjects were examined with isotropic DWI. Nineteen regions of interest (ROIs) were systematically placed, and apparent diffusion coefficients (ADCs) were computed and correlated with T2 and DWI signal intensity in each ROI.**

***RESULTS*: T2 signal abnormalities were always present in territories of the posterior circulation. Anterior circulation structures were involved in 91% of patients. ADC values in areas of abnormal T2 signal were high. More extensive T2 signal abnormalities were seen in patients with a poor outcome than in patients who recovered. In six patients (27%), areas of high DWI signal intensity were seen with ADC values that were paradoxically normal, which we called pseudonormalized. Abnormal T2 signal intensity and high ADC values surrounded these areas. Follow-up images in two patients showed progression to infarction in pseudonormalized regions.**

***CONCLUSION*: Vasogenic edema in PRES involves predominantly the posterior circulation territories, but anterior circulation structures are also frequently involved. The extent of combined T2 and DWI signal abnormalities correlate with patient outcome. High DWI signal intensity and pseudonormalized ADC values are associated with cerebral infarction and may represent the earliest sign of nonreversibility as severe vasogenic edema progresses to cytotoxic edema.**

Posterior reversible encephalopathy syndrome (PRES), hypertensive encephalopathy, reversible posterior cerebral edema syndrome, and posterior reversible leukoencephalopathy are all terms that have been used to describe a group of disorders that present clinically with headache, seizures, visual changes, altered mental status, and occasionally focal neurologic signs (1–5). CT and MR imaging typically show symmetrically distributed areas of vasogenic edema predominantly within the territories of the posterior circulation (1–11) (Fig 1). The abnormalities affect primarily the white matter, but cortex is also involved (1–10, 12). Localized mass effect (1, 5) and subtle enhancement (4, 6, 10) within the lesions have been described, but are not seen consistently. Previous studies (2, 5–7) have shown that vasogenic edema account for the changes observed in PRES. A breakdown in cerebral autoregulation results in the leakage of fluid into the interstitium, which is detected as vasogenic edema (1–11).

When promptly recognized and treated, the symptoms and radiologic abnormalities can be completely reversed (1–8). When unrecognized, the patient's condition can progress to ischemia, massive infarction, and death (5–7, 10, 13, 14). Diffusion-weighted MR imaging (DWI) has been shown to be reliable in distinguishing vasogenic edema in PRES from cytotoxic edema in the setting of cerebral ischemia (2, 5, 7). It stands to reason that DWI could be used to monitor for ischemia as a complication of PRES.

Received November 30, 2001; accepted after revision February 26, 2002.

From the Department of Diagnostic Radiology, Mayo Clinic, Rochester, MN.

Presented in part at the 39th Annual meeting of the American Society of Neuroradiology, Boston, MA, 2001.

Address reprint requests to Patrick H. Luetmer, MD, Department of Diagnostic Radiology, Mayo Clinic, East 2, 200 1st St SW, Rochester, MN 55905.

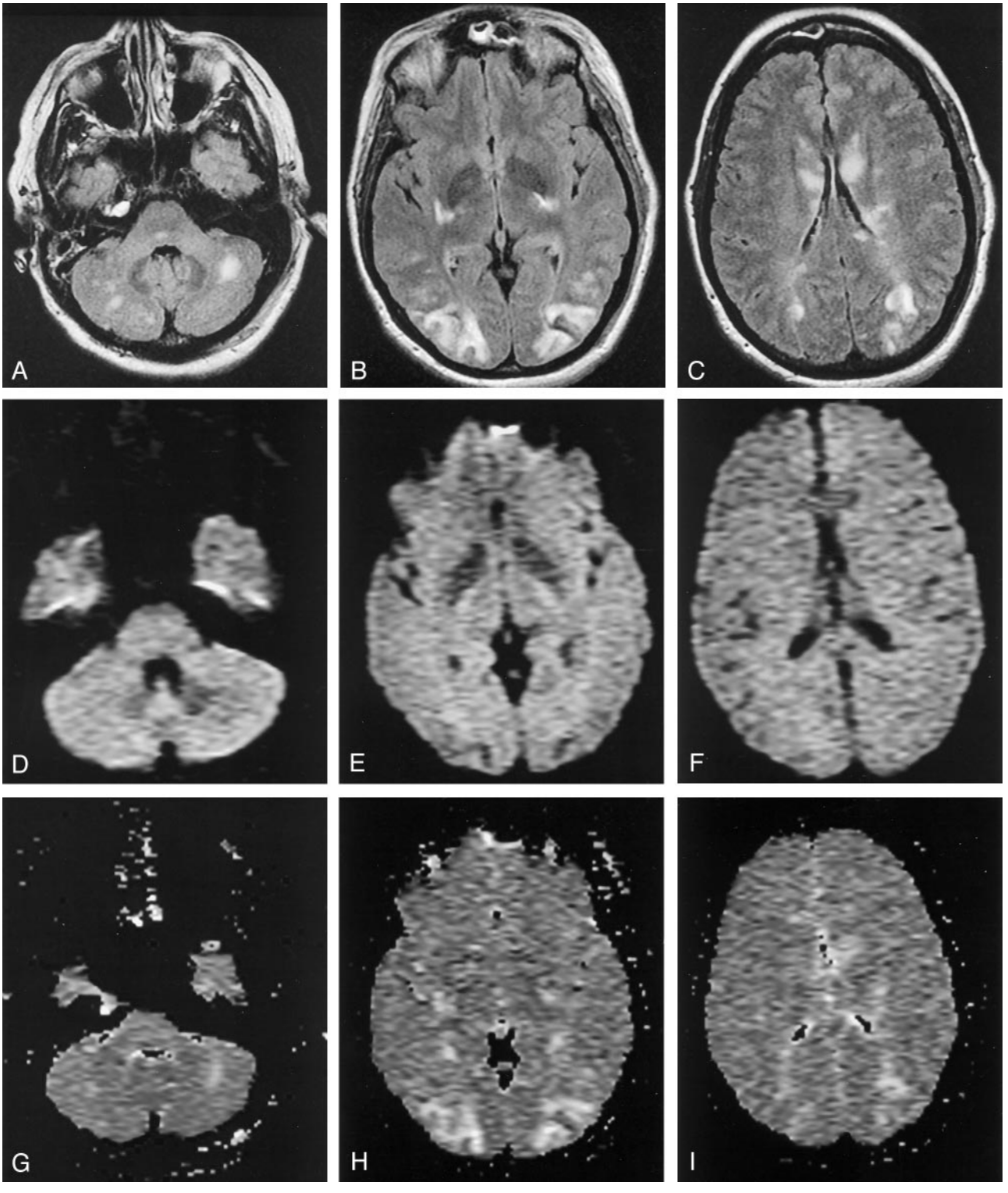

FIG 1. PRES in a pregnant woman with eclampsia (patient 21).

A–C, Axial fluid-attenuated inversion recovery (FLAIR) MR images (TR/TE/TI/NEX, 11,002/140/2250/1; FOV, 20) show symmetric abnormal signal intensity, primarily in the territories of the posterior circulation. The affected area predominantly involves the white matter, but cortex is also involved. Note the involvement of the caudates, which was unusual in our series.

D–F, Isotropic diffusion-weighted MR images (TR/TE, 10,000/91.7; FOV, 40; b = 1,000 s/mm^2) show low to normal signal intensity in the areas of the FLAIR abnormality.

G–I, ADC maps show increased values in the areas of FLAIR abnormality.

A few case reports (5, 10, 13, 14) have described cytotoxic edema as a complication of PRES. Our experience suggests this is a more common complication.

We hypothesized the following: 1) that the extent of regional involvement by vasogenic edema in PRES has prognostic implications and can help in identifying patients who need more aggressive treatment, 2) that severe vasogenic edema can progress to cytotoxic edema, and 3) that DWI can help in predicting the conversion to infarction and irreversible tissue damage.

Methods

We retrospectively identified patients with PRES who underwent brain MR imaging studies at Mayo Clinic during the 36-month period from May 1998 to May 2001. Four inclusion criteria were used: 1) an acute presentation with headache, seizure, visual changes, altered mental status, or focal neurologic signs; 2) the presence of a known risk factor for PRES, such as hypertension, eclampsia, antirejection therapy, uremia, or hemolytic-uremic syndrome; 3) MR examination with findings consistent with PRES; 4) acquisition of diffusion-weighted images.

We searched the clinical record for information on blood pressure (BP), laboratory data, and duration of symptoms in all patients. BP was recorded at the time of presentation and at baseline. Baseline BP was obtained from visits at least 2 months prior to presentation. If the event occurred during hospitalization and if wide fluctuations in BP occurred with hypotension followed by rebound hypertension (eg, sepsis), the baseline BP was defined as the minimum BP value preceding the event. The percentage increase from baseline was calculated by determining the ratio of mean arterial pressure (MAP) at presentation over the baseline value. MAP was calculated by using the following standard formula: MAP = [systolic BP + 2(diastolic BP)]/3. Detailed records from outside institutions were unavailable in two patients (patients 18 and 21), and an appropriate baseline BP could not be obtained.

Serum creatinine and blood urea nitrogen (BUN) levels at the time of the event were recorded for all patients. Serum levels of immunosuppressant agent were obtained in patients receiving antirejection medication. Laboratory markers of endothelial damage, including peripheral smear results, red blood cell morphology, and lactate dehydrogenase (LDH) and uric acid values, were recorded when they were available.

The time between symptom onset and MR imaging was recorded. The length of time that the patient was vulnerable to PRES was also noted, which was defined as the longer of 1) the duration of neurologic symptoms or 2) the time to correction of the underlying cause of the syndrome (eg, time to correct BP, time to stop antirejection medication, time to dialysis).

MR images were obtained by using 1.5-T units capable of producing gradients as high as 40 mT/m. In all patients, T1-weighted sagittal images (TR/TE/NEX, 583/4/1; FOV, 20) and T2-weighted axial images (TR/TE_1, TE_2/NEX, 2033/30, 80/1; FOV, 20) were obtained by using 5-mm sections with a skip of 1 mm and 2.5 mm, respectively. FLAIR images (TR/TE/TI/NEX, 11,002/140/2250/1; FOV, 20, 5-mm-thick contiguous sections) were acquired in all patients but two (patients 13 and 19). In 18 patients these images were obtained in the axial plane, and in two patients (patients 3 and 8), FLAIR images were obtained in the coronal plane. Echo-planar T2- and diffusion-weighted images were obtained with diffusion gradients in the x, y, and z planes by using 5-mm-thick sections with skip of 2.5 mm (TR/TE, 10,000/91.7; FOV, 40; b = 0 and 1,000 s/mm^2). A FLAIR preparation pulse (TI = 2200 ms) was used in all but seven patients (patients 4–6, 11, 14–16). Composite isotropic diffusion-weighted images and apparent diffusion coefficient (ADC) maps were created in all patients by using commercially available software on a separate workstation. In 15 patients (patients 1–6, 9, 11, 12, 14–18), axial and coronal T1-weighted images (TR/TE/NEX, 400/20/2; FOV, 20; section thickness, 5 mm; skip, 2.5 mm) were obtained after the intravenous administration (0.1 mmol/kg) of gadolinium-based contrast material.

Eighteen control subjects who underwent DWI as part of a clinical examination were recruited if they met the following inclusion criteria: 1) the indication was headache, transient ischemic attack, or seizure, and 2) no imaging abnormalities were noted, or the examination showed only minimal leukoariosis or atrophy. Sagittal T1-weighted, axial T2-weighted, axial FLAIR, and diffusion-weighted images were obtained as previously described herein. Diffusion-weighted images were obtained after a FLAIR preparation pulse (TI = 2200 ms) in seven control subjects and without a FLAIR preparation pulse in 11.

For all patients and controls, one of the authors (D.J.C.) systematically placed 19 regions of interest (ROIs) in the cerebellar hemispheres; pons; lenticular nuclei; corticospinal tracts; thalami; and posterior temporal, frontal, parietal, and occipital lobes (Fig 2). These regions were chosen to include cortex, deep gray matter nuclei, and subcortical and deep white matter. The ROIs were placed on the echo-planar T2-weighted images to facilitate correct anatomic placement. The images were then coregistered to the ADC map. Care was taken to avoid including CSF or areas of hemorrhage in the ROI. The mean two-point ADC in each region was measured by using commercial software. Typical ROI sizes were 60–500 mm^2 and varied depending on the brain region studied (Fig 2).

To measure extent of disease, one of the authors (D.J.C.) subjectively graded T2 and FLAIR signal intensity in each region on a scale of 0–3. Normal findings were scored as 0, faint or small areas of signal intensity abnormality were scored as 1, easily perceptible abnormalities were scored as 2, and large confluent areas of high-signal-intensity abnormality on T2-weighted and FLAIR images were scored as 3. A score of 4 was assigned to each region with high DWI signal intensity. We defined the total T2/DWI score for each patient as the sum of the scores in each region. In the patients with high DWI signal intensity, 60-mm^2 ROIs were placed in the areas of abnormal cortex and in the surrounding subcortical white matter.

Patient data were segregated into two groups: normal and abnormal, depending on whether abnormal signal intensity was present on the coregistered echo-planar T2-weighted images (scores 1–3). Patients' ADC values in normal and abnormal areas were then compared with those of control subjects. A two-tailed Student *t* test was used when data were parametrically distributed, and a Wilcoxan rank sum test was used when the data were nonparametrically distributed. Nonparametrically distributed data were seen in the pons (abnormal vs control [A/C] and normal vs control [N/C]), left lenticular nucleus (N/C), right corticospinal tract (N/C), left corticospinal tract (A/C), bilateral thalami (A/C), bilateral occipital lobes (A/C), left frontal lobe (N/C), bilateral parietal lobes (A/C), and bilateral temporal lobes (A/C).

Results

A total of 34 patients with PRES were identified, 22 of whom underwent diffusion-weighted imaging (Table, available at *www.ajnr.org*). The patients were aged 4–90 years (mean age, 45 years) and included 13 female and nine male patients. Seven cases involved hypertensive encephalopathy; eight, antirejection medication toxicity; four, uremia; two, eclampsia; and one, hemolytic-uremic syndrome.

In four patients, a combination of factors that may have led to PRES were present, and we used the patient's clinical presentation to determine which fac-

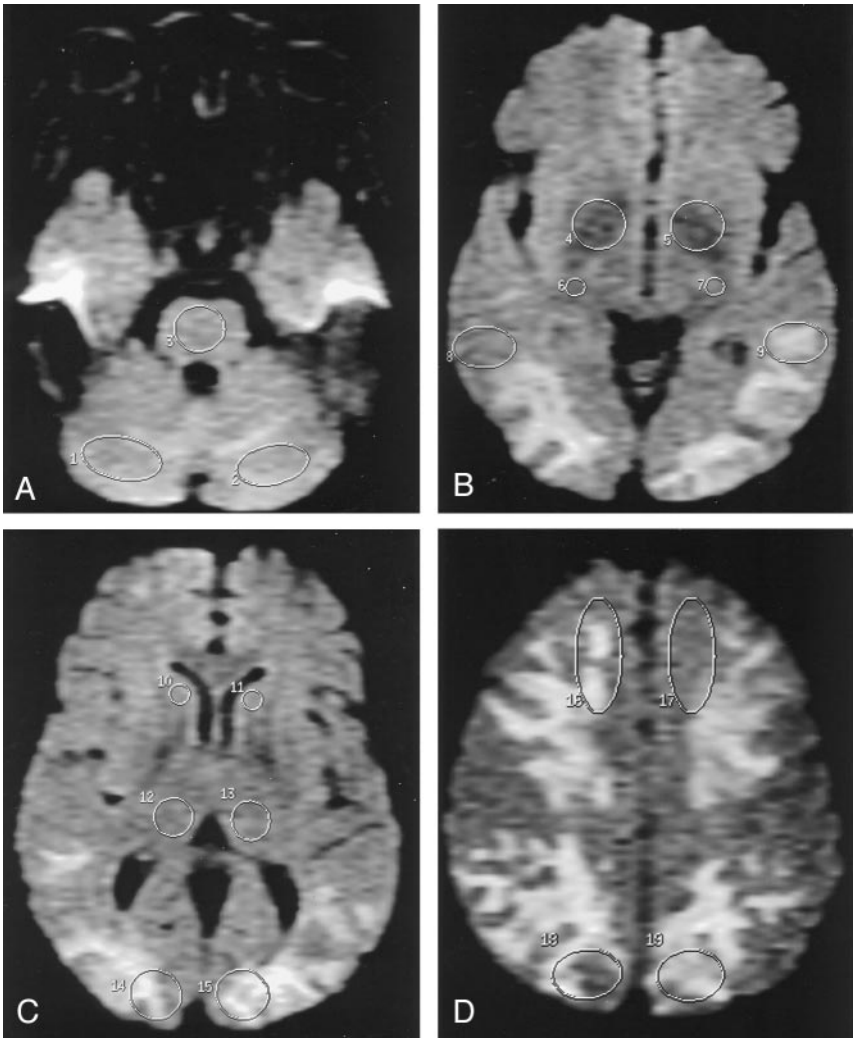

FIG 2. ROI placement. Axial FLAIR-prepped echo-planar T2-weighed images (TR/TE/TI, 10,000/91.7/2200; FOV, 40; b = 0 s/mm^2) in a patient with PRES secondary to uremic encephalopathy (patient 17). Nineteen ROIs were systemically placed in 22 patients with PRES and 18 control subjects, as shown. The images were coregistered to the ADC map, on which measurements were taken. Typical ROI sizes varied with brain region, as follows: cerebellum, 400 mm^2; pons, 240 mm^2; lenticular nucleus, 250 mm^2; corticospinal tract, 60 mm^2; posterior temporal lobe, 360 mm^2; caudate head, 60 mm^2; thalamus, 220 mm^2; occipital lobe, 360 mm^2; parietal lobe, 400 mm^2; frontal lobe, 500 mm^2.

tor was most relevant. Patients 11 and 15 were classified as having antirejection medication neurotoxicity because they responded clinically to a discontinuation of the drug or lowering of the dose, although other factors such as uremia and elevated BP readings may have played a role. Patient 6 presented with an elevated BP after a 3-week period of visual hallucinations and a slow deterioration in his mental status. One week after admission, acute renal failure developed and the BUN level increased. The patient's neurologic symptoms and kidney function recovered after his BP was controlled. The patient was classified as having hypertensive encephalopathy because his symptoms preceded the period of uremia and because he recovered without dialysis. Patient 19 was classified as having uremic encephalopathy because dialysis was necessary to control both her symptoms and her BP, which was labile and which likely contributed to her seizures.

Most patients (63%) underwent imaging within 3 days of symptom onset (Table, available at *www.ajnr.org*). Time between symptom onset and MR examination ranged from 4 hours to approximately 5 months. The 5-month delay followed an extensive workup at an outside institution: repeat MR examination established the diagnosis of PRES. The length of time that patients were vulnerable to PRES ranged from 12 hours to 5 months.

The mean BP elevation from the baseline BP value was 80% (range, 8–158%). In four of our patients (patients 8, 11, 14, 21), no significant elevation in BP from the baseline value was recorded. (The range was 8–29% in three patients; the fourth presented with a BP of 150/70 mmHg and had no prior records.) One of the seven patients (patient 4) who was classified as having hypertensive encephalopathy did not have a systolic BP greater than 200 mmHg. This patient was being treated for sepsis, and wide BP fluctuations were observed (73% above baseline).

In patients with immunosuppressant neurotoxicity, toxic levels of the medication were not required for the development of PRES. Drug levels were elevated in five patients and therapeutic in three. Prior exposure to the medication was not protective: patient 14 had symptoms with therapeutic levels of tacrolimus, even after 5 months of exposure to the drug at similar levels.

Eleven patients in this series had an elevated creatinine level at presentation (patients 5–7, 11, 12, 15–19, 22). Five of the six patients who died (patients

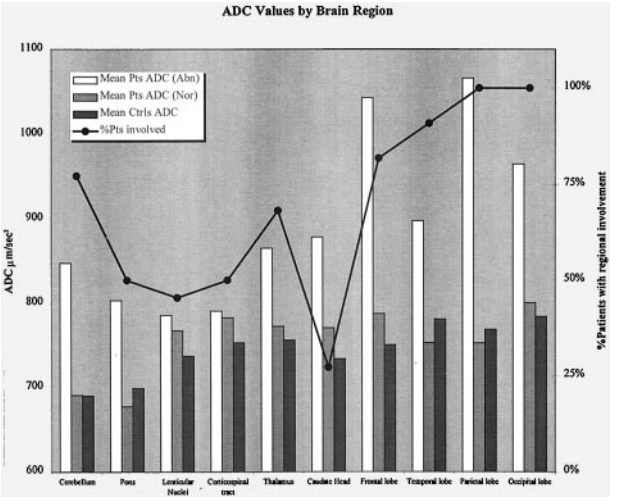

FIG 3. Mean ADC values in brain regions in patients with PRES and control subjects. Percentage of patients with T2 and FLAIR signal intensity abnormalities in each brain region is shown. Both posterior and anterior circulation structures are involved. ADC values in abnormal areas in patients are elevated compared with those in control subjects ($P < .04$); this finding was consistent with vasogenic edema. ADC values in control subjects were lower in the cerebellum and pons ($P < .001$). Mean ADC values from homologous hemispheric structures are averaged together for presentation purposes.

7, 12, 15, 18, 22) had a high creatinine level at presentation (range, 2.7–9.1 mg/dL; mean, 5.1 mg/dL), with a mean elevation of 3.7 mg/dL from the baseline value.

Levels of laboratory markers of endothelial damage were elevated. Among eight patients in whom a peripheral smear was performed, five had shistocytosis, acanthocytosis, or anisocytosis (patients 5, 9, 11, 18, 22). In 14 patients in whom red blood cell morphologic studies were performed, 13 had abnormal morphology (patients 4, 5, 7, 9–13, 15, 16, 18, 19, 22). Serum LDH levels were determined in eight patients (patients 6, 9, 11, 12, 15, 18, 21, 22); these were often elevated, ranging from 161 to 3017 U/L with mean of 726 U/L (normal range, 91–257 U/L). These values are suggestive of shear injury to the circulating red blood cells and are consistent with previously reported results by Schwartz et al (15).

Figure 3 shows the regional distribution of T2 and FLAIR signal intensity abnormalities in our patients. The occipital and parietal lobes were always involved and had some of the highest ADC values, in keeping with the predilection for the posterior circulation territories in PRES. Anterior circulation structures such as the frontal and temporal lobes were also frequently involved (82% and 91%, respectively). Thalamic involvement was seen in 68% patients and pontine involvement, in 50% (Fig 4). ADC values in areas of abnormal T2 signal intensity were consistently elevated compared with those in control subjects ($P < .01$ except for left thalamus and corticospinal tract in which $P = .03$). In patients and controls, findings in the right caudate and corticospinal tract did not differ significantly ($P = .05$ and 0.31, respectively), but these areas were frequently spared. High ADC values are consistent with highly mobile water in areas of vasogenic edema in PRES, as multiple prior studies (2, 5–7) have shown. The majority of the lesions in our patients showed normal or decreased signal intensity with DWI, a phenomenon that Provenzale et al called T2 washout (11).

Interestingly, some of the brain regions that appeared normal on T2-weighted and FLAIR images also showed a tendency to have higher ADC values compared with those in the control subjects. This trend was not statistically significant except in areas that were usually spared on T2-weighted and FLAIR images, such as the left corticospinal tract ($P = .01$) and right and left caudates ($P = .04$ and .02, respectively). This finding suggests that ADC values may be more sensitive to vasogenic edema than findings on conventional T2-weighted and FLAIR images.

Mean ADC values in control subjects were significantly lower in the cerebellum and pons ($P < .001$); this finding may have been due to susceptibility artifact in the skull base or specific properties of the brain tissue in the cerebellum and brain stem.

The extent of disease, as measured with the total T2/DWI score, correlated well with patient outcome. As shown in Figure 5, the patients who had an adverse outcome (stroke or death) had T2/DWI scores that were significantly higher than those of patients who recovered ($P < .001$). Maximum ADC values were also higher among patients with adverse outcomes ($P < .02$), but more overlap was observed between the two groups.

Areas of high DWI signal intensity were observed in six (27%) of 22 patients (patients 4, 6, 11, 14, 15, 18) and were predominantly cortical in distribution. As Figures 6 and 7 demonstrate, these areas had only mildly elevated T2 signal intensity and normal or slightly elevated ADC values; these values were not low, as one would expect in the setting of restricted diffusion in ischemia. We refer to this phenomenon as pseudonormalization of ADC values. The surrounding subcortical white matter consistently showed intensely elevated T2 signal intensity and high ADC values, which were consistent with severe vasogenic edema.

High DWI signal intensity and pseudonormalization were associated with an adverse outcome (two strokes, three deaths) in five of six patients. In patient 11, follow-up T2-weighted and FLAIR images obtained 28 days after the initial examination showed increased signal intensity corresponding to the area of abnormal findings with DWI at presentation (Fig 6). Gyriform, increased T1 signal intensity and subtle enhancement on follow-up images were present; this finding was consistent with petechial hemorrhage into a subacute infarct. The patient recovered quickly after cyclosporin was withdrawn. In patient 6, follow-up MR images obtained 25 days after the onset of symptoms showed gliosis and small foci of cortical enhancement in the right occipital lobe; again, these were consistent with subacute infarction. He recovered after a long period of inpatient rehabilitation.

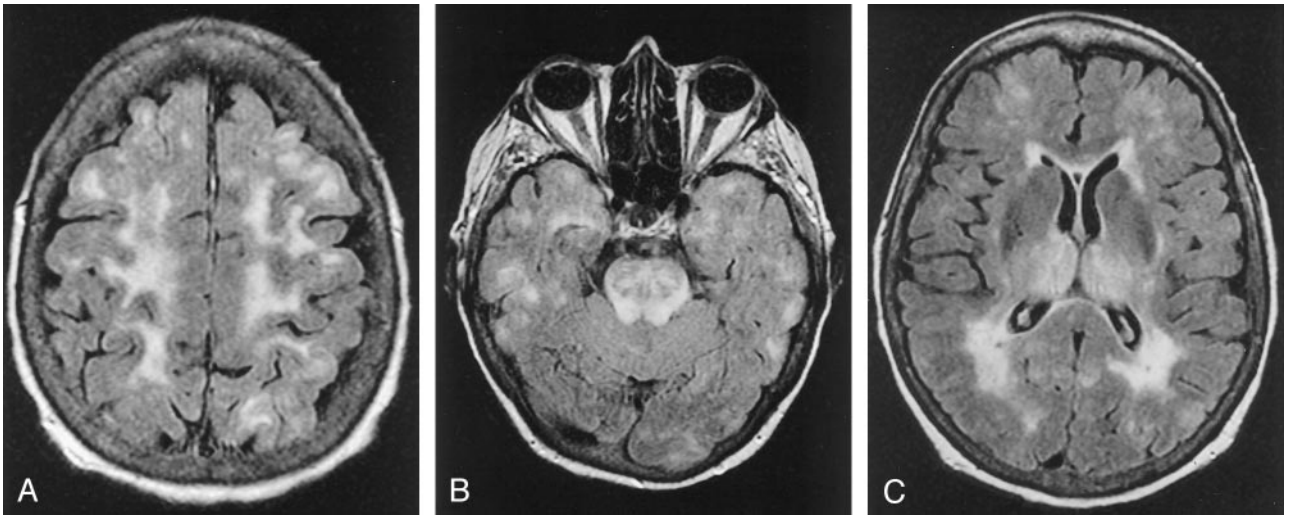

FIG 4. Atypical cases of PRES.

A, Axial FLAIR MR image in a case of uremic encephalopathy (patient 18) shows marked frontal lobe involvement.

B and *C*, Axial FLAIR MR images (TR/TE/TI/NEX, 11,002/140/2,250/1; FOV, 20) in a case of hemolytic-uremic syndrome (patient 22) show involvement in the temporal lobes and thalami. Note also the striking involvement of the brain stem.

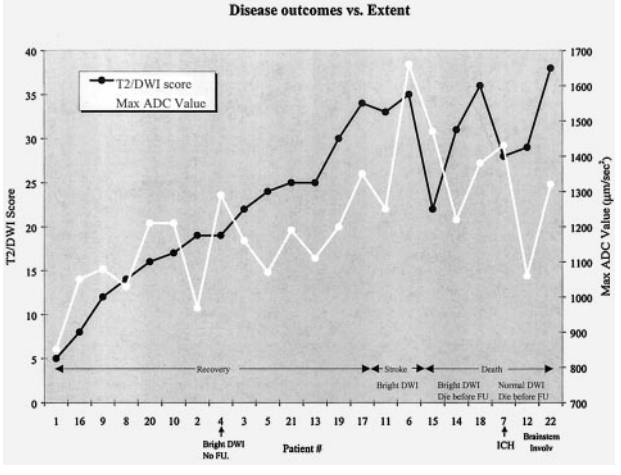

FIG 5. In patients who had an adverse outcome (stroke or death), T2/DWI scores ($P < .001$) and ADC values ($P < .02$) were consistently higher than those of patients who recovered. Patient 4 had cortical DWI hyperintensity at presentation. The patient then recovered and was subsequently lost to follow-up. Patients 6 and 11 had cortical DWI hyperintensity with progression to stroke at follow-up. Patients 14, 15, and 18 had cortical DWI hyperintensity and died before follow-up. Patient 7 had foci of intracranial hemorrhage at presentation. Patients 12 and 22 had severe brain stem PRES.

Three patients (patients 14, 15, 18) with high DWI signal intensity died before follow-up MR imaging could be performed. Patient 15 died of massive aspiration 1.5 months after the initial MR examination. Although patient 14 partially recovered initially and was able to follow simple commands, his neurologic condition again deteriorated after tacrolimus was restarted following retransplantation for hepatic arterial thrombosis. Repeat MR imaging was attempted, but findings were nondiagnostic because of motion. The patient died 2 months after retransplantation, which was 4 months after the first MR examination. Although extensive comorbidities related to his complicated posttransplantion course limited the neurologic assessment and our ability to image him, postulating that PRES played a role in the patient's outcome seems reasonable. Patient 18 had a fulminating clinical course with seizures complicated by respiratory and cardiac arrest, which confounded the findings. MR examination showed changes of watershed infarction superimposed on the changes of PRES. One of the infarcts in the right occipital lobe had the typical appearance of pseudonormalization. Interestingly, areas of watershed infarction in the frontal lobes also exhibited pseudonormalization due to superimposed vasogenic edema.

The only patient with high DWI signal intensity and pseudonormalization who recovered (patient 4) was lost to follow-up. She was discharged 10 days after the MR examination. She had some residual proximal muscle weakness and was instructed to undergo follow-up MR imaging in 2–3 months and to consult a local neurologist.

Two patients (patients 12 and 22) had severe brain stem involvement, with a score of 3 in the pons, and neither survived. In patient 12, the response to gradual tapering of cyclosporin was poor, with persistently decreased mental status and repeated episodes of seizures. This patient died 38 days later after supportive measures were withdrawn at the request of the family. Patient 22 also did not recover neurologically despite rapid control of her BP, and she died 3 days after the MR examination. Of the two patients with a pontine score of 2, one (patient 18) also had areas of high DWI signal intensity elsewhere and died, and the other (patient 19) recovered within 24 hours of the onset of symptoms, after aggressive intervention with dialysis. Subtle increased T2 signal intensity in the pons (score = 1) was not clearly associated with a bad outcome, as four of seven patients (patients 5, 10, 13, 21) recovered fully. No patients in our series had areas of high DWI signal intensity in the brain stem.

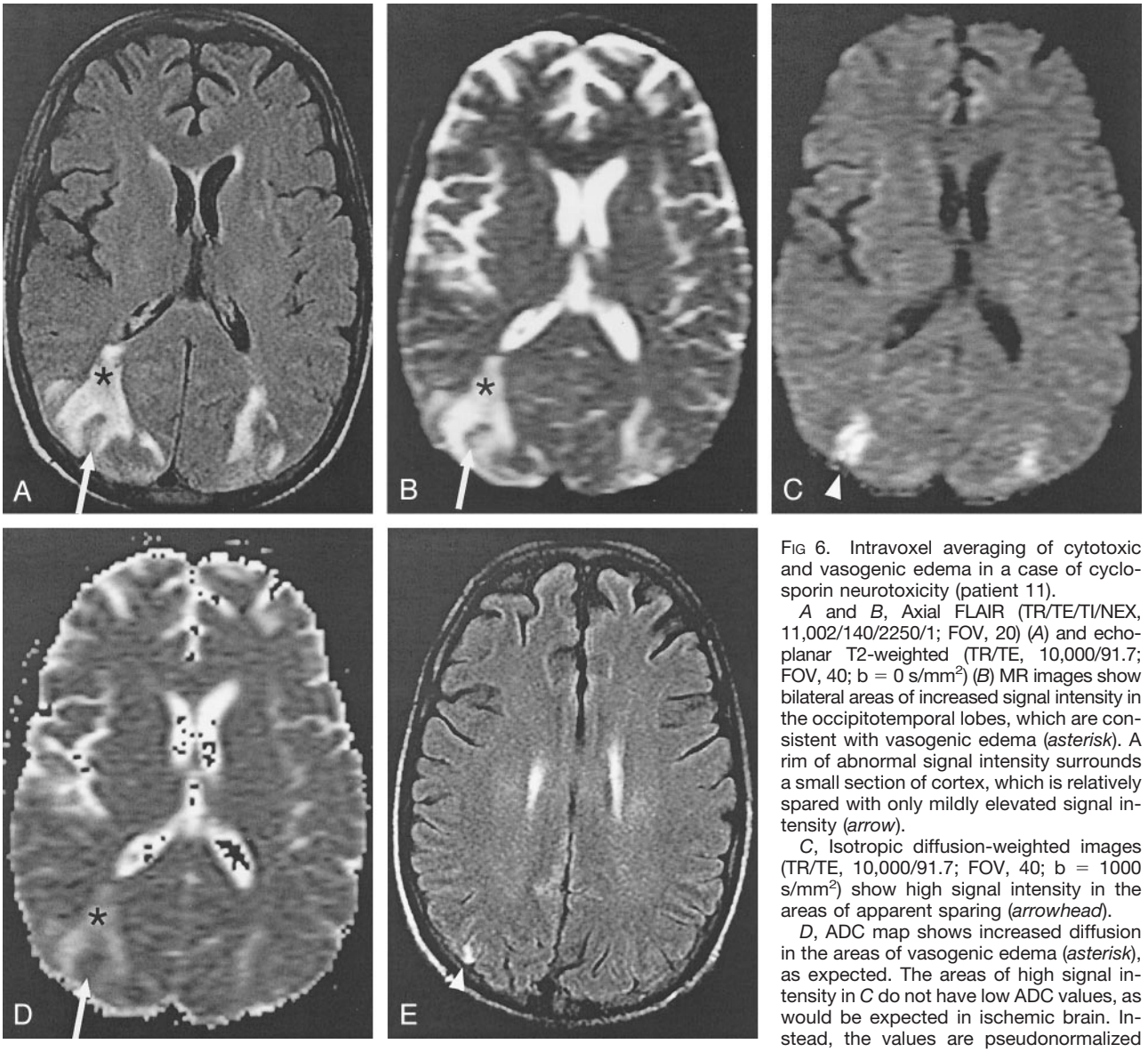

FIG 6. Intravoxel averaging of cytotoxic and vasogenic edema in a case of cyclosporin neurotoxicity (patient 11).

A and *B*, Axial FLAIR (TR/TE/TI/NEX, 11,002/140/2250/1; FOV, 20) (*A*) and echo-planar T2-weighted (TR/TE, 10,000/91.7; FOV, 40; b = 0 s/mm^2) (*B*) MR images show bilateral areas of increased signal intensity in the occipitotemporal lobes, which are consistent with vasogenic edema (*asterisk*). A rim of abnormal signal intensity surrounds a small section of cortex, which is relatively spared with only mildly elevated signal intensity (*arrow*).

C, Isotropic diffusion-weighted images (TR/TE, 10,000/91.7; FOV, 40; b = 1000 s/mm^2) show high signal intensity in the areas of apparent sparing (*arrowhead*).

D, ADC map shows increased diffusion in the areas of vasogenic edema (*asterisk*), as expected. The areas of high signal intensity in *C* do not have low ADC values, as would be expected in ischemic brain. Instead, the values are pseudonormalized (*arrow*).

E, Follow-up FLAIR image obtained 28 days later shows increased signal intensity (*arrowhead*) corresponding to the region of abnormal findings at DWI. Gyriform, increased T1 signal intensity and subtle enhancement (not shown) was also present; this finding is consistent with petechial hemorrhage into a subacute infarct (not shown).

T1-weighted, T2-weighted, and echo-planar T2-weighted images depicted foci of intracranial hemorrhage in two patients (9%; patients 7, 8). In both patients, platelet counts assessed at the time of presentation were within the normal range (276×10^9/L and 361×10^9/L). Patient 7 was hypertensive at presentation with a BP of 200/106 mmHg and a 58% elevation from her baseline BP (Table, available at *www.ajnr.org*). Patient 8, a 9-year-old boy, was also hypertensive for his age, with a BP of 140/70 mmHg. He was able to recover after the withdrawal of cyclosporin.

Gadolinium enhancement in the areas of T2 abnormality was an inconsistent finding in our series, seen in only five (33%) of 15 patients (patients 5, 6, 11, 12, 20) who received contrast material at presentation.

Discussion

PRES is a remarkably heterogeneous group of disorders. In patients with hypertensive encephalopathy and in pregnant patients with eclampsia (2, 4, 6–9, 13–16), PRES is thought to occur after a subacute elevation in BP. In the transplant population, PRES is a well-known complication of antirejection therapy with cyclosporin A and tacrolimus (1, 4, 8, 10, 12, 17–20). It is also seen in the setting of uremia, hemolytic-uremic syndrome, and thrombotic thrombocytopenia purpura, in which endothelial toxins are thought to play a role (2, 8, 21). PRES has also been reported in association with chemotherapeutic agents such as cisplatin (22), interferon alpha (4), intrathecal methotrexate (23), and multidrug treatment of acute lymphoblastic leukemia in children (14, 24). PRES-

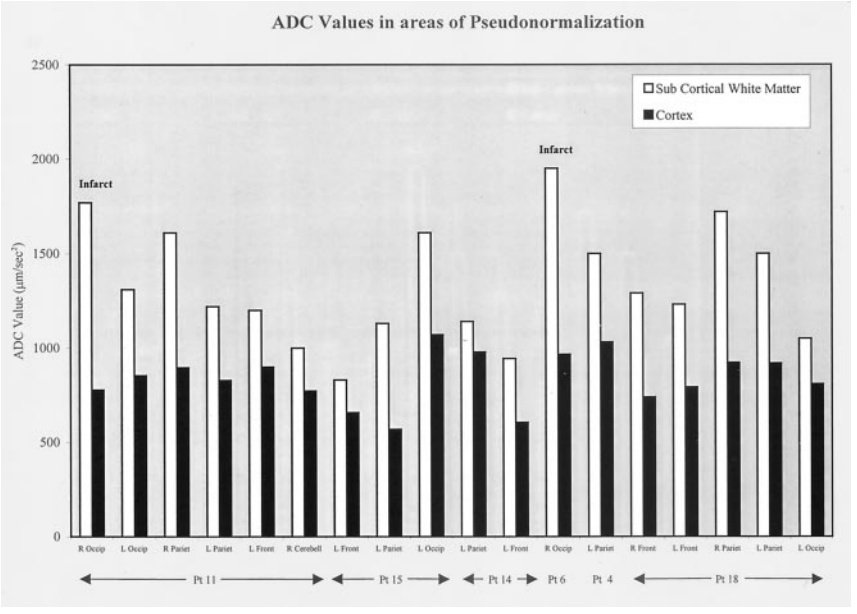

FIG 7. ADC values in areas of pseudonormalization. High values were seen in the subcortical white matter and pseudonormalized values were seen in the cortex. Pseudonormalization results from intravoxel averaging of vasogenic and cytotoxic edema in cortex. In two patients, follow-up images confirmed the development of infarcts in areas of pseudonormalization.

like abnormalities have also been described in patients with acute intermittent porphyria (25) and cryoglobulinemia (26).

The predilection for involvement of posterior circulation territories is generally accepted to result from the relatively sparse sympathetic innervation of the vertebrobasilar circulation (27). In a healthy subject, cerebral autoregulatory mechanisms that have both myogenic and neurogenic components maintain constant brain perfusion (15). The effectiveness of the neurologic component of autoregulation is directly proportional to the degree of sympathetic innervation (28). In patients with PRES, the myogenic response is blunted by either passive overdistention of the vessel due to elevations in BP (2, 5–10) or direct toxic effects on the endothelium (15, 17). Because autoregulatory mechanisms are thus more dependent on the neurogenic response, the more poorly innervated areas in the posterior circulation are most vulnerable. The result is the leakage of fluid into the interstitium and vasogenic edema (1–10, 15).

The findings in our series confirm the predilection for posterior circulation territories in PRES, but not to the exclusion of anterior circulation structures. Frontal lobe involvement was seen in 82% of patients and was often striking (Fig 4). Furthermore, our data suggest that quantitative analysis of ADC maps may show subtle involvement with PRES that goes undetected with conventional MR imaging. The clinical utility of this observation is unclear because obvious T2 signal intensity abnormalities elsewhere were present in all of our patients by virtue of the retrospective nature of the study. Perfusion MR imaging studies designed to identify asymptomatic patients who are taking immunosuppressants and who may be at risk for PRES have, so far, failed in detecting subclinical lesions in these patients (29). Further studies are needed to ascertain whether quantitative analysis of ADC maps can be used for this purpose. Regardless, these subtle changes in quantitative ADC maps indicate that the pathophysiology of this phenomenon may be more global than previously thought. If severe enough, even the more richly innervated territories of the anterior circulation become vulnerable to PRES.

We observed areas of cortical DWI hyperintensity in 27% of our patients, an incidence that was much higher than those of previous reports. Instead of the low ADC values one would expect in the setting of ischemic injury with irreversible damage, ADC values in areas of cortical DWI hyperintensity were pseudonormalized. We postulate that the paradoxically normal or elevated ADC values in areas of DWI hyperintensity result from intravoxel averaging of both cytotoxic and vasogenic edema in cortex affected by PRES. Because restricted diffusion in cytotoxic edema lowers ADC values and vasogenic edema elevates them, the effects cancel each other out when the two combine at the subvoxel level.

This concept can be illustrated schematically by using the Stejskal-Tanner equation (30), which states that the magnitude of the diffusion signal S is governed by the following equation: $S = S_0e^{-bD}$, where S_0 is the signal at $b = 0$ s/mm^2 (ie, echo-planar T2-weighting image signal intensity), b is the gradient b value, and D is the ADC. In the logarithmic plot of S versus b (Fig 8), the slope of the line is equal to the value plotted on the ADC map, and the magnitude of the signal intensity at $b = 1000$ s/mm^2 equals the value plotted on the DWI image. In vasogenic edema, the slope of the signal intensity is steep due to the high mobility of water molecules, and at $b = 1000$ s/mm^2, the magnitude of the signal intensity decreases below the level in the normal case. This effect results in high ADC values with normal DWI signal intensity, as shown in Figure 1D–I. In areas of pseudonormalization, acute infarction occurs in the presence of vasogenic edema so that the net diffusion signal in-

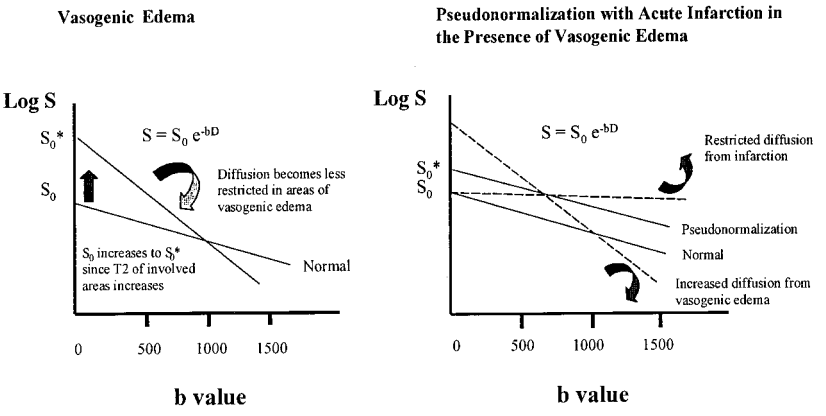

FIG 8. Schematic representations of the diffusion signal intensity in vasogenic edema and pseudonormalization in cortex affected by PRES. By definition, the slope of the signal intensity is plotted on the ADC map, and the magnitude of the signal intensity at b = 1,000 s/mm^2 is plotted on the diffusion-weighted image.

A, Vasogenic edema. Because water is highly mobile in areas of vasogenic edema, the slope of the signal intensity is steeper and the ADC values are higher, as shown in Figure 1G–I. At b = 1000 s/mm^2, the magnitude of the diffusion signal intensity is either normal or below normal, as shown in Figure 1D–F.

B, Pseudonormalization. The net diffusion signal intensity results from averaging of a cytotoxic component, which has restricted water motion and therefore has a shallow slope, and a vasogenic component, with a steep slope. The net diffusion signal intensity line is parallel to the normal case but higher in magnitude. Because the slopes are parallel, ADC values are isointense or normal in the areas of pseudonormalization, as shown in Figure 6D. Because the magnitude is higher at b = 1000 s/mm^2, the DWI signal intensity is high, as shown in Figure 6C.

tensity results from the averaging of a cytotoxic component, which has restricted water motion and therefore has a shallow slope, and a vasogenic component with a steep slope. The net diffusion signal intensity line is parallel to that in the normal case but higher in magnitude. Because the slopes are parallel, ADC values are isointense relative to those of normal tissue in the areas of pseudonormalization, as shown in Figure 6D. Because the magnitude is higher at b = 1000 s/mm^2, the DWI signal intensity is high, as shown in Figure 6C.

This model also explains the appearance of the areas of pseudonormalized cortex on echo-planar T2-weighted images. In vasogenic edema, S_0 is high because increased water content in the interstitium increases T2 signal intensity. In pseudonormalization, the cytotoxic component of the signal contributes little to S_0 because T2 signal intensity in ischemic tissue is isointense in the first 6–8 hours (31). Therefore, because S_0* in pseudonormalized tissue is the average of S_0 for vasogenic edema and S_0 for cytotoxic edema, S_0* in pseudonormalized tissue results in a modest increase in T2 signal intensity lower than that in the surrounding areas of vasogenic edema (Fig 8). Furthermore, more compaction of cells in the cortex also likely damages the effect of vasogenic edema on S_0*, because the cortex probably allows less vasogenic edema than does adjacent white matter.

The notion that cortical high DWI signal intensity in PRES is due to cytotoxic edema is supported by our patients' clinical outcomes. Two of the six patients with high DWI signal intensity progressed to infarction, as was shown on follow-up images. High DWI signal intensity was associated with a poor prognosis, with death as the outcome in three of the remaining patients, and infarction conceivably contributed to the patients' outcomes. The patient who was lost to follow-up had subtle residual neurologic deficits 10 days later, and that she may have had a small infarct seems a reasonable explanation.

An alternative explanation is that cortical-restricted diffusion abnormalities in PRES may be reversible until the effects of cytotoxic edema begin to dominate and ischemia may ensue. This suggestion may be supported by the observation that, in patient 11, only the area with the highest difference in ADC value between cortex and surrounding subcortical white matter progressed to ischemia, and follow-up images did not show evidence of infarction in the other areas of pseudonormalization. Further prospective studies are needed to clarify the precise temporal evolution of ischemia in PRES. Such a prospective study would ideally include a perfusion sequence to assess differences in cerebral blood flow in areas of uncomplicated vasogenic edema versus areas of pseudonormalization.

The progression to subacute infarction that we observed in areas of cortical DWI hyperintensity is consistent with prior case reports of PRES in the literature. Ay et al's (5) original description of cytotoxic edema in a patient with PRES showed large areas of restricted diffusion 3 days prior to their patient's demise. Koch et al (13) describe a case in which areas of cytotoxic edema in PRES led to tissue loss on follow-up images obtained 2 months later. Interestingly, they also report high ADC values (980 μm/s^2) in the region of increased diffusion signal intensity, as we noted in our patients. Cooney et al (14) observed gliosis, white matter volume loss, and petechial hemorrhage on follow-up images that corresponded to areas of high DWI signal intensity at presentation.

The mechanism by which vasogenic edema in PRES becomes cytotoxic is not well understood. Ay et al (5) suggest that, in areas of massive vasogenic edema, increased tissue pressure eventually impairs the microcirculation and leads to ischemia. Localized mass effect is a common finding in PRES and was present to some degree in all six patients with pseudonormalization. Animal studies (32) have shown that the breakdown in autoregulatory mechanisms in hypertensive encephalopathy precedes the development of decreased cerebral blood flow and stroke. In our patients, cytotoxic edema developed in cortex immediately adjacent to areas with intensely elevated ADC values in the subcor-

tical white matter; this finding is consistent with a heavy burden of fluid in the interstitium. The postulation that unchecked vasogenic edema results in cytotoxic edema and infarction seems reasonable.

Increased DWI signal intensity without T2 abnormality has been reported in the setting of sustained seizure activity (33). Findings of animal studies suggest that the diffusion abnormalities appear within 1 hour of persistent seizure activity and precede the development of irreversible T2 signal abnormalities (34). Although seizures were a common presenting symptom in our series, no seizure activity was reported in four of the six patients (patients 6, 11, 14, 15) with restricted diffusion. Of the remaining two patients, one (patient 4) had two short witnessed episodes of seizures within a 24-hour period, but no evidence of status epilepticus was present. Seizure activity seems unlikely to have played a large role in the pathogenesis of DWI abnormalities in these patients.

Even in the absence of high DWI signal intensity, severe vasogenic edema was associated with a poor prognosis in our patients. Extensive involvement with PRES, as measured by high T2/DWI scores, was seen in all patients who died, including the three patients who died despite their having no DWI abnormalities at presentation. Two of these patients had severe brain stem involvement, and one had intracranial hemorrhage. It seems reasonable that both hemorrhage and brain stem involvement indicate severe PRES that will respond poorly to treatment. Published case reports (20, 35) of severe PRES involving the brain stem have involved at least partial recovery, but in those cases, reversible T2 abnormality was isolated to the brain stem. Our patients had lesions in the pons in the context of generalized PRES involving supratentorial structures; therefore, extrapolating our findings to this variant of the syndrome is difficult. Larger studies are needed to establish the precise relationship of brain stem involvement to patient outcome.

In our series, frank intracranial hemorrhage was associated with hypertension, not thrombocytopenia. Findings in the 9-year-old child with a BP of 140/90 mmHg in whom intracranial hemorrhage developed are consistent with the observations of Jones et al (9) that children are vulnerable to PRES and its complications at BPs lower than those of adults. They postulate that cerebral autoregulatory mechanisms in children are left-shifted to function at lower BPs.

High T2/DWI scores were also observed in a few of the patients who recovered; the clinical circumstances can account for this finding, at least in part. Patients 17 and 19, for example, had uremic encephalopathy and promptly underwent dialysis at the first sign of symptoms, and their symptoms resolved in 36 and 24 hours, respectively. This finding suggests that a window of opportunity is present after severe PRES is recognized; during this time, immediate intervention can have a substantial clinical effect.

Conclusion

In conclusion, MR imaging with diffusion-weighted sequences provides not only a powerful means of diagnosing PRES but also a wealth of prognostic information about the patient. The hallmark of this diagnosis is vasogenic edema in the territories of the posterior circulation, which can be reliably differentiated from cytotoxic edema in other etiologies by using DWI and by calculating the ADC map, which shows elevated ADC values. Involvement of anterior circulation structures is also common and should not deter consideration of this diagnosis. Diffusion-weighted images may show foci of high signal intensity in cortex that is either undergoing infarction or at high risk of infarction. ADC values in these areas are normal or slightly elevated. We call this finding pseudonormalization and propose that it results from intravoxel averaging of values in cytotoxic and vasogenic edema. We suggest that this finding may represent an early sign of nonreversibility in PRES, heralding the conversion to infarction. The extent of T2 and DWI signal intensity correlates well with patient outcome and can help guide more aggressive treatment in more severely affected patients. Intracranial hemorrhage and brain stem involvement were also associated with a poor prognosis.

Acknowledgements

The authors would like to thank Mr Scott Harmsen and Mr Jeffrey Harrington for their assistance with the statistical analysis.

References

1. Casey SO, Sampaio RC, Michel E, Truwit CL. **Posterior reversible encephalopathy syndrome: utility of FLAIR imaging in the detection of cortical and subcortical lesions.** *AJNR Am J Neuroradiol* 2000;21:1199–1206
2. Schwartz RB, Mulkern RV, Gudbjartsson H, Jolesz F. **Diffusion-weighted MR imaging in hypertensive encephalopathy: clues to pathogenesis.** *AJNR Am J Neuroradiol* 1998;19: 859–862
3. Dillon W, Rowley H. **The reversible posterior cerebral edema syndrome.** *AJNR Am J Neuroradiol* 1998;19:591
4. Hinchey J, Chaves C, Appignani B, et al. **A reversible posterior leukoencephalopathy syndrome.** *N Engl J Med* 1996;334:494–500
5. Ay H, Buonanno FS, Schaefer PW et al. **Posterior leukoencephalopathy without severe hypertension: utility of diffusion-weighted MRI.** *Neurology* 1998;51:1369–1376
6. Schwartz RB, Jones KM, Kalina P, et al. **Hypertensive encephalopathy: findings on CT, MR imaging and SPECT imaging in 14 cases.** *AJR Am J Roentgenol* 1992;159:379–383
7. Schaefer PW, Buonanno FS, Gonzalez RG, Schwamm LH. **Diffusion-weighted imaging discriminates between cytotoxic and vasogenic edema in a patient with eclampsia.** *Stroke* 1997;28:1082–1085
8. Port J, Beauchamp N. **Reversible intracerebral pathologic entities mediated by vascular autoregulatory dysfunction.** *Radiographics* 1998;18:353–367
9. Jones BV, Egelhoff JC, Patterson RJ. **Hypertensive encephalopathy in children.** *AJNR Am J Neuroradiol* 1997;18:101–106
10. Mukherjee P, McKinstry RC. **Reversible posterior leukoencephalopathy syndrome: evaluation with diffusion-tensor imaging.** *Radiology* 2001;219:756–765
11. Provenzale JM, Petrella JR, Celso LH, Wong JC, Engelter S, Barboriak DP. **Quantitative assessment of diffusion abnormalities in posterior reversible encephalopathy syndrome.** *AJNR Am J Neuroradiol* 2001;22:1455–1461
12. Schwartz RB, Bravo SM, Klufas RA, et al. **Cyclosporin neurotoxicity and its relationship to hypertensive encephalopathy: CT and MR findings in 16 cases.** *AJR Am J Roentgenol* 1995;165:627–631
13. Koch S, Rabinstein A, Falcone S, Forteza A. **Diffusion-weighted imaging shows cytotoxic and vasogenic edema in eclampsia.** *AJNR*

Am J Neuroradiol 2001;22:1068–1070
14. Cooney MJ, Bradley WG, Symko SC, et al. **Hypertensive encephalopathy: complication in children treated for myeloproliferative disorders—report of three cases.** *Radiology* 2000;214:711–716
15. Schwartz RB, Feske SK, Polak JF, et al. **Preeclampsia-eclampsia: clinical and neuroradiologic correlates and insights into the pathogenesis of hypertensive encephalopathy.** *Radiology* 2000;217:317–376
16. Sanders TG, Clayman DA, Sanchez-Ramos L, et al. **Brain in eclampsia: MR imaging with clinical correlation.** *Radiology* 1991; 180:475–478
17. Truwit CL, Denaro CP, Lake JR, DeMarco T. **MR imaging of reversible cyclosporin A-induced neurotoxicity.** *AJNR Am J Neuroradiol* 1991;12:651–659
18. Jansen O, Krieger D, Krieger S, Sartor K. **Cortical hyperintensity on proton-weighted images: an MR sign of cyclosporin-related encephalopathy.** *AJNR Am J Neuroradiol* 1996;17:337–344
19. Coley SC, Porter DA, Calamante F, et al. **Quantitative MR diffusion mapping and cyclosporin-induced neurotoxicity.** *AJNR Am J Neuroradiol* 1999;20:1507–1510
20. Oliverio PJ, Restrepo L, Mitchell SA, et al. **Reversible tacrolimus-induced neurotoxicity isolated to the brain stem.** *AJNR Am J Neuroradiol* 2000;21:1251–1254
21. Bakshi R, Shaikh ZA, Bates VE, Kinkel PR. **Thrombotic thrombocytopenic purpura: brain CT and MR findings in 12 patients.** *Neurology* 1999;52:1285–1288
22. Ito Y, Arahata Y, Goto Y et al. **Cisplatin neurotoxicity presenting as reversible posterior leukoencephalopathy syndrome.** *AJNR Am J Neuroradiol* 1998;19:415–417
23. Yaffe K, Ferreiro D, Barkovich JA, Rowley H. **Reversible MRI abnormalities following seizures.** *Neurology* 1995;45:104–107
24. Shin RK, Stern JW, Janss AJ, et al. **Reversible posterior leukoencephalopathy during the treatment of acute lymphoblastic leukemia.** *Neurology* 2001;56:388–391
25. Kupferschmidt H, Bont A, Schnorf H, et al. **Transient cortical blindness and bioccipital brain lesions in two patients with acute intermittent porphyria.** *Ann Intern Med* 1995;15:598–600
26. Hodson AK, Doughty RA, Norman ME. **Acute encephalopathy, streptococcal infection, and cryoglobulinemia.** *Arch Neurol* 1978; 35:43–44
27. Edvinson L, Owman C, Sjoberg NO. **Autonomic nerves, mast cells, and amine receptors in human brain vessels: a histochemical and pharmacological study.** *Brain Res* 1976;115:337–393
28. Beausang-Linder M, Bill A. **Cerebral circulation in acute arterial hypertension: protective effects of sympathetic nervous activity.** *Acta Physiol Scand* 1981;111:193–199
29. Sheth TN, Ichise M, Kucharczyk, W. **Brain perfusion imaging in asymptomatic patients receiving cyclosporin.** *AJNR Am J Neuroradiol* 1999;20:853–856
30. Stejskal EO, Tanner JE. **Spin diffusion measurements: spin echoes in the presence of a time-dependent field gradient.** *J Chem Phys* 1965;42:288–292
31. Gonzalez RG, Schaefer PW, Buonanno FS, et al. **Diffusion-weighted MR imaging: diagnostic accuracy within 6 hours of stroke symptom onset.** *Radiology* 1999;210:155–162
32. Tamaki K, Sadoshima S, Baumbach GL, Iadecola C, Reis DJ, Heistad DD. **Evidence that disruption of the blood-brain barrier precedes reduction in cerebral blood flow in hypertensive encephalopathy.** *Hypertension* 1984;6:I75–I81
33. Kassem-Moussa H, Provenzale JM, Petrella JR, Lewis DV. **Early diffusion-weighted MR imaging abnormalities in sustained seizure activity.** *AJR Am J Roentgenol* 2000;174:1304–1306
34. Nakasu Y, Nakasu S, Morikawa S, Uemura S, Inubushi T, Handa J. **Diffusion-weighted MR in experimental sustained seizures elicited with kainic acid.** *AJNR Am J Neuroradiol* 1995;16:1185–1192
35. de Seze J, Mastain B, Stojkovic T, et al. **Unusual MR findings of the brain stem in arterial hypertension.** *AJNR Am J Neuroradiol* 2000; 21:391–394